SIMULATION OF DEPOSITION AND ACTIVITY DISTRIBUTIONS OF RADIONUCLIDES IN HUMAN AIRWAYS

Á. Farkas[1], I. Balásházy[1], I. Szőke[1], W. Hofmann[2] and R. Golser[2]

[1]Radiation and Environmental Physics Department, KFKI Atomic Energy Research Institute,
P.O. Box 49, H-1525 Budapest 114, Hungary
[2]Institute of Physics and Biophysics, University of Salzburg,
Hellbrunner Str. 34, A-5020 Salzburg, Austria

INTRODUCTION

The aim of our research activities is the modelling of the biological processes related to the development of lung cancer at the large central-airways observed in the case of uranium miners caused by the inhalation of radionuclides (especially alpha-emitting radon decay products).

Statistical data show that at the uranium miners the lung cancer has developed mainly in the 3-4-5th airway generations and especially in the right upper lobe. Therefore, it is rather important to study the physical and biological effects in this section of the human airways to find relations between the radiation dose and the adverse health effects.

These results may provide useful information about the validity or invalidity of the currently used LNT (Linear-No-Threshold) dose-effect hypothesis at low doses.

In the frame of these activities the first step is the accurate modeling of airway-geometry and the simulation of regarded flow fields. On the basis of flow field calculations trajectories of the inhaled radionuclides can be calculated in order to simulate their deposition on the inner side of the airways. Taking into account the coordinates of the deposited particles, local deposition patterns can be computed. The primary distribution of deposition may be significantly effected by the clearance pattern. Having modeled the deposition patterns and flow of the mucus layer, activity distributions of the deposited radon progenies are computed.

GEOMETRY MODELS AND COMPUTATIONAL MESHES

The flow field of the inhaled aerosols as well as the deposition patterns of inhaled particles and the related biological effects strongly depend on the geometry of airways. Therefore, we study the effect of geometry on the flow field in single and multiple tracheo-bronchial airway bifurcations.

Earlier geometric models for the simulation of airflow patterns in human airway bifurcations were generally restricted either to a two-dimensional problem [1], [2], [3] or to a three-dimensional approach without a defined central transition zone [4]. In our simulations, we apply the three-dimensional “narrow” and “wide” idealized geometric models introduced by Balásházy and Hofmann [5,6] and the a morphologically realistic bifurcation, “MRB”, model [7], which is the mathematically further developed so called physiologically realistic bifurcation, "PRB", model of Heistracher and Hofmann [8]. This model assures smooth

transitions between the airways and may have a curved carina. The surface is described mathematically and one of our computer programs provides input data for the UNIGRAPHICS code, which is an advanced CAD/CAM/CAE solid modeling and engineering program. The 3D geometry is then exported into the GAMBIT software to be meshed.

The most significant difference between the idealized ("narrow" and "wide" geometries) and the "MRB" (morphologically realistic bifurcation) model is the shape of the carinal ridge and the smooth transitions between the branches. The wedge shaped carinal region of the "narrow" and "wide" bifurcations is replaced by a curved, more realistic surface in case of the MRB model (Fig. 1).

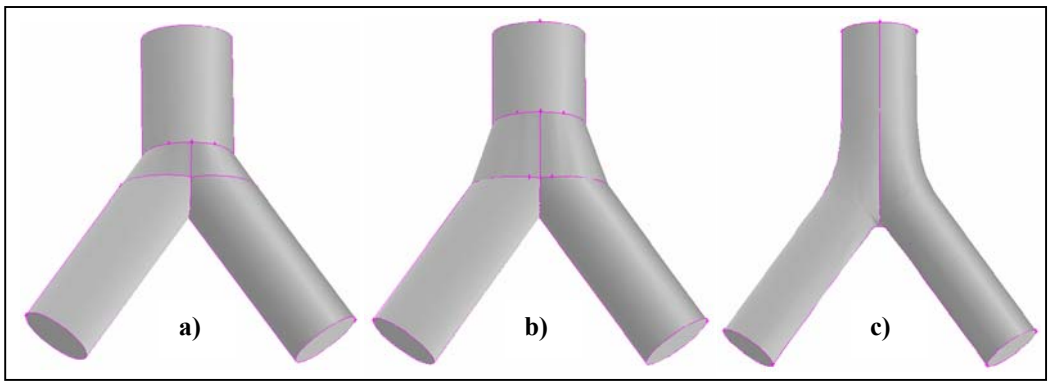

Fig. 1 Bifurcation geometry models: a) "narrow", b) "wide", c) "MRB"

Inasmuch as we perform numerical computations, the created geometry must be meshed to obtain a numerical grid. The structure of the mesh may influence the flow calculation and particle trajectory results, therefore the construction of an adequate computational grid is important. During the mesh construction we had to take into account on the one hand the limits of the capacity of our computers, on the other hand the necessity of a high cell density to reach accurate results. Therefore we constructed an inhomogeneous mesh, which is denser where the velocity gradient is enhanced (near the walls) and where we expect high local deposition density values (central region, inner part of daughter branches, upper and lower sides of the parent branch). Figure 2 shows the main characteristics of our mesh in case of a simple "narrow" bifurcation.

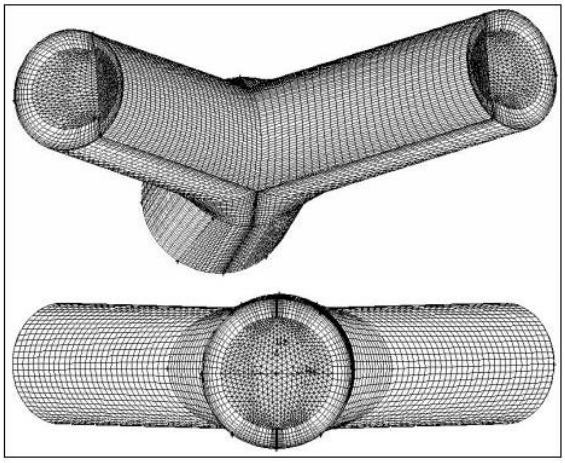

Fig. 2 The numerical mesh used for airflow and trajectory calculations.

In addition, FLUENT has also a grid adaptation option. It means that the cells of the mesh can be divided into finer cells where the velocity gradient is high and cells can be merged where the gradient is low. However, we will apply it with the parallel observation of cell degeneration because this operation may produce the degeneration of cells if the grid adaptation is not used carefully.

FLOW FIELD COMPUTATIONS

Due to the complexity of the geometry, a numerical approach must be applied. Analytical models can only be appropriate if the bifurcation geometry and the flow field are strongly idealized, such as the assumption of straight tube geometry with uniform or parabolic flow or bent tube with rotational flow. A detailed description of the problems associated with the application of analytical approaches can be found in several publications e.g. [9-12].

In our most recent efforts, we applied a numerical approach for the computation of flow field by the FLUENT CFD code. Here, the airflow is computed solving the Navier-Stokes and continuity equations in a three-dimensional computational mesh by a finite volume method. Where necessary, an under-relaxation technique is used in order to speed up the convergence procedure.

Setting of the boundary conditions is a vital step of the numerical computation. At the inlet, the velocity field is characterized by a parabolic profile. This profile is produced by a UDF (User Defined Function), which can be interpreted and linked by the compiler built into the FLUENT. It is practically impossible to measure the local pressure distribution in airway bifurcations [13]. Therefore at the outlets constant pressure condition is applied. Constant pressure condition calls forth that the ratio of flow rates in the daughter branches is equal with the ratio of the cross-sections of the outlets. No experimental evidence is available which justifies the application of a pressure boundary condition other than constant.

Applying the above-described computational method, inspiratory and expiratory flow patterns were computed at different flow rates. The results strongly depend on the shape of the geometry. One can observe that the shape of the central zone significantly influences the flow field both for inspiration and expiration (Fig. 3).

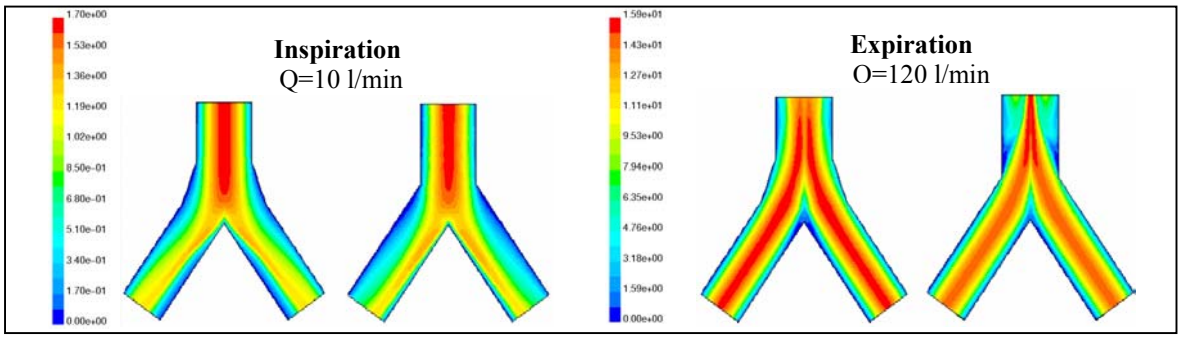

Fig. 3 Flow fields for "narrow" and "wide" bifurcation models at 10 l/min flow rate, inspiration (left panel) and 120 l/min flow rate, expiration (right panel).

These differences in geometry and flow field influence the deposition of inhaled aerosol particles and the related health effects. Due to the stronger secondary velocity components in the vicinity of the dividing spur at "narrow" bifurcation, it is very likely that for this geometry the deposition is more intense on the inner part of the daughter branches during inspiration than at wide or MRB geometries.

Computed flow patterns (Fig. 4) and consequently the deposition of particles strongly depend on the flow rate. A comprehensive study about the health effects of inhaled radionuclides requires the application of wide range of flow rates from 10 l/min (sleeping breathing condition) to 120 l/min (heavy exercise).

In order to highlight the main characteristics of the realistic flow field in this section of the tracheo-bronchial tree, time dependent flow field computations were also performed. Currently, only a few studies are available in the literature regarding unsteady flow simulations in airways [14,15].

For time dependent flow computations sinusoidal inlet pressure and constant outlet pressure conditions were assumed. The breathing conditions were set to 60 l/min flow rate and 15 min^{-1} breathing frequency. The numerical time step was 0.05 s. In Figure 5, some flow patterns during the inhalation and some during the exhalation period are displayed during the second breathing cycle.

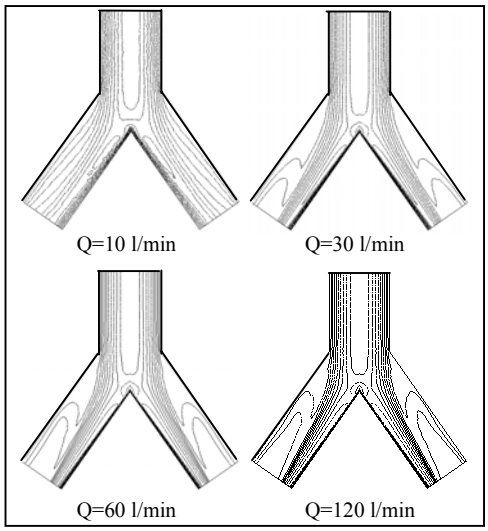

Fig. 4 Flow fields at airway generations 3-4 at different tracheal flow rates. In each contour representation 10 velocity isolevels are displayed; a) Q=10 l/min; b) Q=30 l/min; c) Q=60 l/min; d) Q=120 l/min.

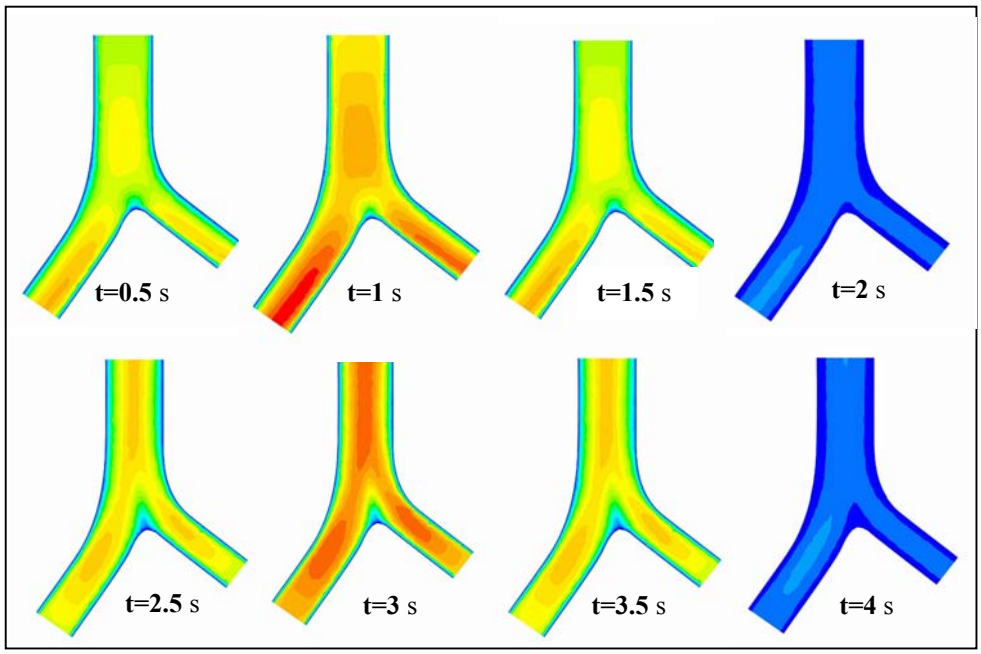

Fig. 5 Some time dependent flow patterns in an asymmetrical bifurcation at 60 l/min flow rate during the second breathing cycle, inhalation (upper panel), exhalation (bottom panel), breathing cycle is 4 s.

PARTICLE TRAJECTORIES AND DEPOSITION PATTERNS

After the flow simulations, trajectories of the inhaled radionuclides have been calculated taking into account the main deposition mechanisms, characteristics in human airways: inertial impaction, gravitational settling and Brownian motion. To perform these computations a user enhanced trajectory model of the FLUENT CFD (Computational Fluid Dynamics) code has been applied.

The solver uses a numerical integration method (iteration algorithm) in order to solve the particle force balance equation and track the trajectory of the injected particles [16]. The distribution of the randomly injected spherical particles follows the inlet velocity profile. In order to create this injection an own code has been applied. Particles intersecting the wall zone, are trapped by the mucus layer and deposit.

Particle trajectories have been computed for a large range of flow rates (10 l/min, 30 l/min, 60 l/min and 120 l/min) and particle sizes (1 nm, 10 nm, 100 nm, 1 μm and 10 μm).

In Fig. 6, trajectories of inhaled radionuclides in an airway bifurcation, colored by velocity magnitudes are displayed.

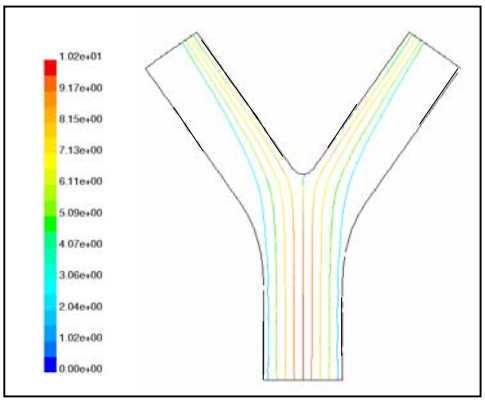

Fig. 6 Trajectories of inhaled particles in a symmetrical MRB bifurcation model.

Coordinates of particle trajectory endpoints can be written out from the solver memory applying compiled UDF (User Defined Functions). Plotting of this dotes provide us the deposition patterns.

Our earlier aerosol deposition studies, Fig. 7, have demonstrated that deposition patterns of inhaled aerosols within airway bifurcations are distinctly inhomogeneous both during inhalation and exhalation. Our present deposition patterns confirm these findings.

Primary “hot spots” were found in the vicinity of the carina for all particle sizes during inhalation. The deposition is more pronounced at the inner side of the daughter branches in case of inspiration and at the upper and lower sides of the parent branch in case of expiration.

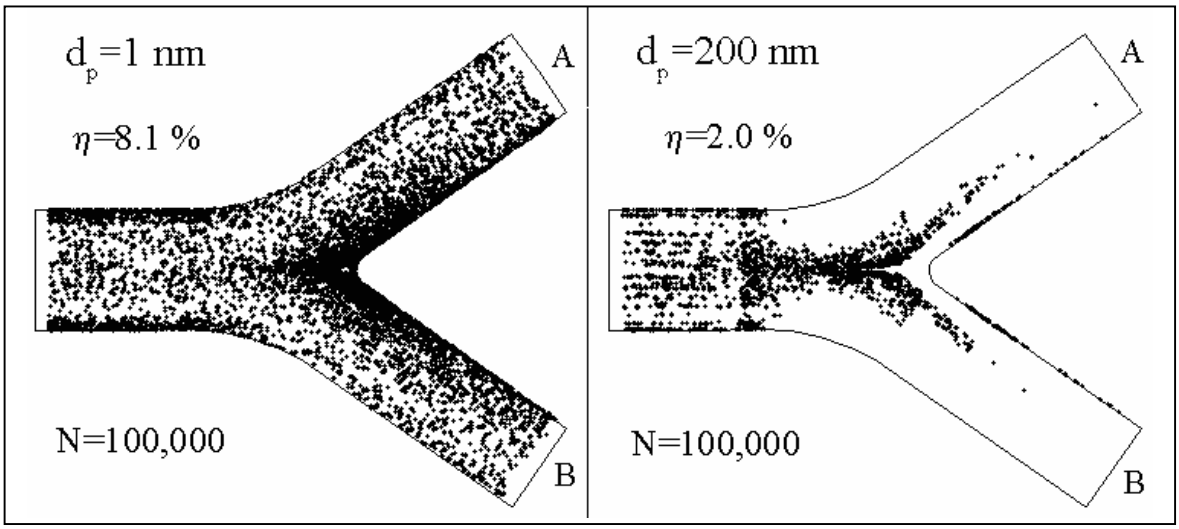

Fig. 7 Deposition patterns of 1nm and 200 nm particles during inhalation at 60 l/min flow rate in an MRB bifurcation, d_p: particle size, η: deposition efficiency, N: number of particles.

For the quantification of the deposition in a section of the airways the deposition efficiency, as the ratio of the deposited and selected particles at the proper inlet, can be computed. The deposition efficiency values in different generations for different flow rates and particle parameters may serve as important parameter for further studies. Some calculated deposition efficiency data in the 3-4th generation of the human tracheo-bronchial tree are presented in Table 1.

Geometry	**flow rate** (l/min)	**particle diameter** (μm)	**deposition efficiency** (%)
Narrow	60	1	2.4
Narrow	60	0.001	9
Narrow	60	0.01	3.1
Narrow	60	10	42
MRB	60	1	2.1
MRB	60	0.001	8.1
MRB	60	0.01	2.3
MRB	60	10	45
Narrow	10	0.01	2.5
Narrow	10	1	1
Narrow	10	10	13.4
MRB	10	0.01	1.7
MRB	10	0.001	14
MRB	10	1	1.1
MRB	10	10	4

Table 1. Deposition efficiencies for different geometries and particle sizes in airway generations 3-4, parabolic inlet profile, branching angle 35 degree.

The above displayed deposition efficiency values were computed for a whole but single bifurcation. As the deposition is not homogenous local deposition density values have been also computed.

Before the computation of the activity distributions, we have studied the effect of the main clearance mechanism, that is, the velocity distributions of the mucus layer along the airway bifurcations by the FLUENT CFD code, because the activity distributions depend on the residence times of the deposited particles. Our modelling efforts regarding the mucociliary clearance, which is the main clearance mechanism in this section of the airways [17], show a strongly reduced clearance velocity in the vicinity of the peak of the carina. This phenomenon may further increase the asymmetry of the primary deposition patterns.

For the computation of the exact activity distributions we consider booth the attached and unattached fractions of radon progenies.

CONCLUSIONS

In this paper, the first steps to a comprehensive mechanism based dose-effect relationship study are presented in the filed of lung dosimetry, where not the determination of the average cellular doses but the distributions of the cellular burdens are characterised.

One of the largest available dose – effect databases are the results of the radon studies at high, intermediate and low doses. Thus, we have focused our simulation efforts to the characterisation of the elemental biophysical processes at the inhalation of radon and its progenies. Our results suggest strong dependency of airflow, particle deposition and activity distributions on the airway geometry, flow rate and particle size. The biological response must be also sensitive to these parameters.

Finding the relationship between the inhaled cellular burden and the related health effects in the lung at different doses and breathing parameters, may serve as a big step for the support or rejection of the LNT (Linear No Threshold) hypothesis.

ACKNOWLEDGEMENTS

This research was supported by the Hungarian OTKA T030571, T034564, NKFP-3/005/2001 and NKFP-1/008/2001 Projects, and by the CEC Contract No. FIGD-CT-2000-00053, FIS5-2002-000016 and FIGM-CT-2000-50001 Projects.

REFERENCES

1. Ferron, G.A., Hillebrecht, A., Peter, J., Priesack, E., Thoma, M., Kuenzer, I.., Mederer, Rand Klump, U. G. *Airflow simulation in two dimensional bifurcations*, J. Aerosol Sci., **22**, Suppl. 1, S 809-812 (1991).
2. Lee, J. W. and Goo, J. H. *Numerical simulation of airflow and inertial deposition of particles in a bifurcating channel of square cross section.* J. Aerosol Med., **5** (3), 131-154 (1992).
3. Martonen, T.B., Zhang, Z. and Lessmann, R.C., *Fluid dynamics in the human larynx and upper tracheobronchial airways*. J. Aerosol. Sci. Technol. **19**, 133-156 (1993).
4. Kinsara, A. A., Tompson, R. V. and Loyalka, S. K., *Computational flow and aerosol concentration profiles in lung bifurcations*. Health Phys. **64** (1), 13-22 (1993).

5. Balásházy, I. and Hofmann, W., *Particle deposition in airway bifurcations-I.: Inspiratory flow*. J. Aerosol Sci. **14** (6), 745-772 (1993).
6. Heistracher, T. and Hofmann, W. *Physiologically realistic models of bronchial airway bifurcations.* J. Aerosol Sci. **26**, 497-509 (1995).
7. Balásházy, I., Hofmann, W. and Martonen, T.B. *Inertial impaction and gravitational deposition of aerosols in curved tubes and airway bifurcations*. Aerosol Sci. and Technol. **13,** 308-321 (1990).
8. Balásházy, I., Hofmann, W. and Martonen, T.B. *Inspiratory particle deposition in airway bifurcation models.* J. Aerosol Sci. **22,** 15-30 (1991).
9. Hofmann, W. and Balásházy, I. *Particle deposition patterns within airway bifurcations - solution of the 3D Navier-Stokes equation.* Rad. Prot. Dos. **38,** 57-63 (1991).
10. Kim, C.S. and Iglesias, A.J., *Deposition of inhaled particles in bifurcating airway models.* J. Aerosol Med. **2** (1), 1-14 (1989).
11. Pedley, T.J. *Pulmonary fluid dynamics*. Ann. Rev. Fluid Mech. **9**, 229-274 (1977).
12. Balásházy I. *Simulation of particle trajectories in bifurcating tubes.* J. Comput. Phys. **110**, 11-22 (1994).
13. Balásházy, I. and Hofmann, W. *Deposition of aerosols in asymmetric airway bifurcations.* J. Aerosol Sci. **26,** 273-292 (1995).
14. George A. Ferron, David A. Edwards *Numerical simulation of air and particle transport in the conducting airways.* J. Aerosol Med., **3** (9), 303-316.
15. Z. Zhang, C. Kleinstreuer, C.S.Kim *Cyclic micron-size particle inhalation and deposition in a triple bifurcation lung airway model.* J. Aerosol Sci. **33**, 257-281 (2002).
16. Fluent 6.0 User's Guide, Volume 4, 19. Discrete Phase Models. Fluent Inc. 2001.
17. International Commission on Radiological Protection, (1994) Human Respiratory Tract Model for Radiological Protection. Oxford, Pergamon Press, ICRP Publications 66, Ann. ICRP 24.